Formation and Dissociation Kinetics of the Magnesium(II) Complex of 1,4,7-Triazacyclononane-1,4,7-tris(methylenemethylphosphinic acid)

Jurriaan Huskens[†] **and A. Dean Sherry***[,†,‡]

Department of Chemistry, University of Texas at Dallas, P.O. Box 830688, Richardson, Texas 75083-0688, and Department of Radiology, Rogers Magnetic Resonance Center, University of Texas Southwestern Medical Center, 5801 Forest Park Road, Dallas, Texas 75235-9085

Received February 29, 1996[⊗]

The dissociation and the formation rate of the Mg^{II} complex of 1,4,7-triazacyclononane-1,4,7-tris(methylenemethylphosphinate) (NOTMP) have been studied by nonequilibrium potentiometry and ^{31}P NMR spectroscopy. The dissociation reaction was dominated by a proton-assisted pathway in which the complex ML (M = Mg^{II}, L = NOTMP) is protonated to H−ML in a rapid equilibrium (log $K_{H-ML} = 5.2$), which then dissociates to M and HL in a rate determining step ($k_{d,H-ML} = 1.4 \times 10^{-2}$ s^{-1}). The formation reaction appeared to be faster, and the first part of the reaction was dominated by a pathway in which the metal ion rapidly forms a weak complex with the non-protonated ligand (M−L) that slowly rearranges to the final complex ML. The intermediate M−L was not observed directly, but likely involves partial coordination of M to L *via* the phosphinate oxygens. Below pH 7, a proton-assisted pathway prevailed involving a species M−HL (log $K_{M-HL} = 1.79$). This intermediate has a proton attached to a ring nitrogen, while the metal is probably coordinated to the phosphinate oxygens, similar to M−L. An overall reaction scheme was used to simulate all potentiometric pH curves and the NMR titration data. This model shows that, at equilibrium, (de)complexation is dominated by the proton-assisted pathway at pH < 7.0, while above this pH the spontaneous dissociation of ML and the formation of ML from M−L prevail.

Introduction

An assessment of a possible regulatory role[1] for Mg^{II} in isolated cells, perfused organs, or intact tissue has been limited by the availability of direct methods for monitoring levels of free Mg^{II}, $[Mg]_f$. There are currently three common methods for measuring $[Mg]_f$ in biological tissue, using the fluorescent indicator Furaptra[2] or Mg^{II} selective microelectrodes[3,4] or by monitoring the ^{31}P NMR shift differences between the ATP resonances.[5] The first two methods are typically used to measure $[Mg]_f$ in single cells while the third, being less sensitive, requires a large number of cells or a relatively large volume of intact tissue. Other biological cations (H^+, Na^I, K^I, or Ca^{II}) interfere with all three methods with varying degrees. We have recently reported a new ligand, 1,4,7-triazacyclononane-1,4,7-tris(methylenemethylphosphinate) (NOTMP (L)), for monitoring $[Mg]_f$ in biological fluids.[6] The ^{31}P resonances of the free ligand (37.0 ppm) and the Mg^{II} complex (42.5 ppm) were in slow exchange, thus allowing the observation of both resonances separately and providing the ratio of their peak areas by signal integration. The pH 7.4 conditional stability constant, $K_d = [Mg]_f[L]_f/[MgL]$ ($[L]_f = [L] + [HL] + [H_2L]$) was 1.0 mM at 298 K and 0.35 mM at 310 K. Since the latter value is comparable to typical free Mg^{II} concentrations in cells (0.5 mM), the $[MgL]/[L]_f$ ratio and, consequently, $[Mg]_f$ can be monitored accurately using this NMR method. Furthermore, this ligand is quite NMR sensitive because of the three equivalent ^{31}P nuclei and the sharp line widths, and it is selective for Mg^{II} over Ca^{II}.

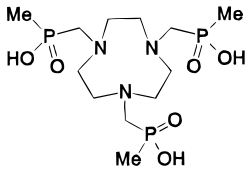

For determination of intracellular Mg^{II} concentrations, for example in perfused hearts, it is important to have an idea of the time scale of complex formation/dissociation. It has been observed[7] that intracellular $[Ca]_f$ oscillates in a beating heart during the period of one beat. Conversely, nothing is currently known about alterations in $[Mg]_f$. A ligand that responds slowly to such changes in free metal ion concentration might bind only that amount of Ca^{II} or Mg^{II} corresponding to the average free metal ion concentration, without further disrupting the dynamics of the organ.

Furthermore, knowledge of the kinetic behavior of macrocyclic ligands in general is quite important in many other areas, including contrast agents for magnetic resonance imaging.[8] For linear aminopolycarboxylate complexes, the formation/dissociation rate depends largely on the exchange rate of water molecules in the first coordination sphere of the metal ion[9] and on the formation of the chelate rings.[10] For macrocyclic ligands, however, the observed rates are usually much lower and depend

* Author to whom correspondence should be sent (either address). Telephone: 214-883-2907 or 214-648-5877. FAX: 214-883-2925 or 214-648-5881. E-mail: sherry@utdallas.edu.
† University of Texas at Dallas.
‡ University of Texas Southwestern Medical Center.
⊗ Abstract published in *Advance ACS Abstracts,* August 1, 1996.

(1) Grubbs, R. D.; Maguire, M. E. *Magnesium* **1987**, *6*, 113−127.
(2) Raju, B.; Murphy, E.; Levy, L. A.; Hall, R. D.; London, R. E. *Am. J. Physiol.* **1988**, *256*, C540−548.
(3) Buri, A.; McGuigan, J. A. S. *Exp. Physiol.* **1990**, *75*, 751−761.
(4) Hu, Z.; Bührer, T.; Müller, M.; Rusterholz, B.; Rouilly, M.; Simon, W. *Anal. Chem.* **1989**, *61*, 574−576.
(5) Gupta, R. K.; Moore, R. D. *J. Biol. Chem.* **1980**, *255*, 3987−3993.
(6) Huskens, J.; Sherry, A. D. *J. Am. Chem. Soc.* **1996**, *118*, 4396−4404.
(7) Harding, D. P.; Smith, G. A.; Metcalfe, J. C.; Morris, P. G.; Kirschenlohr, H. L. *Magn. Reson. Med.* **1993**, *29*, 605−615.
(8) Tweedle, M. F. In: *Lanthanide Probes in Life, Chemical and Earth Sciences*; Bünzli, J.-C. G., Choppin, G. R., Eds.; Elsevier: Amsterdam, 1989.
(9) Choppin, G. R.; Wong, P. J. *ACS Symp. Ser.* **1994**, *565*, 346−360.
(10) Dasgupta, P.; Jordan, R. B. *Inorg. Chem.* **1985**, *24*, 2717−2720. Dasgupta, P.; Jordan, R. B. *Inorg. Chem.* **1985**, *24*, 2721−2723. Voss, R. H.; Jordan, R. B. *J. Am. Chem. Soc.* **1976**, *98*, 6926−6932.

S0020-1669(96)00229-7 CCC: $12.00

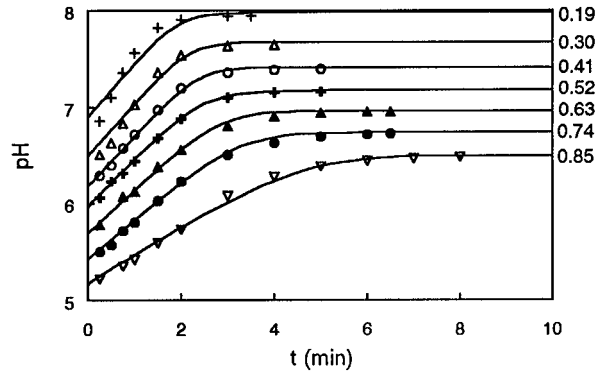

Figure 1. pH *vs* time as a function of $[H]_{tot.}/[L]_{tot.}$ (values shown next to corresponding curves) for the potentiometric titration of 2.7 mM NOTMP + 3.0 mM Mg^{II} with 0.1 M HCl (I = 0.1 M KCl, 298 K). The solid lines were obtained by simulation of the kinetic model shown in Scheme 3.

on a variety of factors including ring size, pK_as and microscopic protonation sequences, hydrogen bridging, and steric hindrance of the side-chains. Therefore, mechanistic details of the reaction of any macrocyclic ligand with metal ions may provide new insights into the general behavior of this class of compounds.

During the performance of the potentiometric titrations for the determination of the stability of Mg(NOTMP),[6] we observed that equilibration generally took a few minutes. In this paper, we report an investigation of the kinetics of this complex, as studied by nonequilibrium potentiometry and ^{31}P NMR spectroscopy. Most kinetic studies employ buffered solutions (the pH-stat technique) or solutions with a known (high) acid concentration. In both situations, the pH is constant and is only varied from experiment to experiment. In this study, the changes of pH with time have been used to monitor the reaction rate, so that additional indicators or buffers were unnecessary.

Experimental Section

Potentiometry. Potentiometric titrations were conducted at 298 K using an Accumet 925 pH meter (Fisher), an Orion 8103 Ross combination electrode and a Metrohm 665 Dosimat automatic burette (Brinkman Instruments). The ionic strength was adjusted to 0.1 M using KCl in all titrations, and all measurements were performed under a N_2 atmosphere. Hydrogen ion activities were obtained from millivolt readings, and the electrode was calibrated using Ricca high precision buffers. Hydrogen ion activities were converted to concentrations using a pK_w of 13.79 (H_2O, 298 K) and an H^+ activity coefficient of 0.82, which were determined from separate titrations of 0.001 and 0.01 M KOH with 0.1 M HCl. pD values for the experiment in D_2O are actual meter readings (uncorrected).

All solutions were prepared from distilled, demineralized, and degassed water and were saturated with and stored under N_2. The dissociation experiment was performed by titrating a 10 mL high pH (10) Mg(NOTMP) solution ($[M]_{tot.}$ = 3.0 mM, $[L]_{tot.}$ = 2.7 mM) with 0.1 M HCl. The HCl aliquot size (0.03 mL) was chosen such that there were seven additions for which $0 < [H]_{tot.}/[L]_{tot.} < 1$ (0.27−0.45 mL HCl). As observed previously in the standard potentiometric titration curve,[6] this was the region in which formation/dissociation takes place. For all additions, the pH was monitored as a function of time until equilibrium was reached (defined as: d(pH)/dt < 0.02 unit/min). The complex formation experiment in H_2O was performed in an analogous way by titrating a low pH (3) Mg(NOTMP) solution with 0.1 M KOH. The experiment in D_2O contained 2.5 mM $K_2HNOTMP\cdot 2KCl\cdot 2H_2O$ plus 3.0 mM $MgCl_2$ in D_2O and was titrated with 0.1 M KOH in D_2O.

NMR Spectroscopy. ^{31}P NMR spectra (202 MHz) were recorded on a General Electric GN500 NMR spectrometer using a 10 mm broad-band probe. Spectra were recorded at 298 K using the standard GN variable temperature control unit. Aqueous 85% phosphoric acid (0 ppm) was used as the external standard, and broad-band ^1H decoupling (WALTZ) was applied.

For the NMR dissociation experiment, the same Mg(NOTMP) solution was used as described above for the potentiometric titrations, to which 5% D_2O was added for locking. A syringe was connected *via* thin tubing to the NMR tube inside the spectrometer, thus allowing acquisition immediately after an addition of HCl. The aliquot size of HCl was adjusted so there were 3 additions for which $0 < [H]_{tot.}/[L]_{tot.} < 1$. Spectra were taken at t = 0.25, 0.5, 1, 1.5, 2, 3, and 5 min, each consisting of 8 acquisitions lasting approximately 10 s. The dissociation experiments in both H_2O and D_2O were performed in an analogous manner.

Calculations. A fitting of the experimental data to various models was performed using a general spreadsheet program, as described earlier.[11] For the potentiometric dissociation experiment (Figure 1), all species concentrations were evaluated, both under equilibrium and initial conditions, using the mass balances shown in eqs 1−3 (ignoring the third protonation step, log K_3 = 2.0). Here, L is NOTMP and M is Mg^{II}.

$$[M]_{tot.} = [M] + [ML] + [H{-}ML] + [M{-}HL] \quad (1)$$

$$[L]_{tot.} = [L] + [HL] + [H_2L] + [ML] + [H{-}ML] + [M{-}HL] \quad (2)$$

$$[H]_{tot.} = [H] - [OH] + [HL] + 2[H_2L] + [H{-}ML] + [M{-}HL] \quad (3)$$

The equilibrium concentrations (Figure 1, Table 2) were obtained as follows. From a first guess for [L], the values of [HL] and $[H_2L]$ were calculated using the protonation constants, K_1 (log K_1 = 10.92) and K_2 (log K_2 = 3.97),[6] where $K_n = [H_nL]/[H_{n-1}L][H]$. Subtracting eq 2 from eq 1 gave [M], and use of β_{MHL} (log β_{MHL} = 12.76)[6] gave [MHL], which is the sum of [M−HL] and [H−ML]. Substitution into eq 1 gave [ML]. Substitution into 3 gave a calculated value for $[H]_{tot.}$, which was used to provide a better estimate for [L] as described previously.[11,12] This loop was continued until calculated and experimental $[H]_{tot.}$ values were equal (relative error < 10^{-8}).

The initial concentrations (Figure 1, Table 1) were obtained as follows: initial pH values (pH_0) were obtained by extrapolation of the linear parts of the curves shown in Figure 1 to t = 0. $K_{M-HL} = 0$ was used as an initial estimate. The sum of the amounts of ML and H−ML at equilibrium must equal the sum of these species at t = 0 after the addition of the next aliquot of titrant, because these species are in rapid equilibrium and it is assumed that no reaction (to M and M−HL) has taken place at t = 0. Similar reasoning is valid for M and M−HL. This leads to eqs 4 and 5 (dilution effects are omitted for clarity), where

$$[M]_0^{i+1} + [M{-}HL]_0^{i+1} = [M]_{eq}^{i} + [M{-}HL]_{eq}^{i} \quad (4)$$

$$[ML]_0^{i+1} + [H{-}ML]_0^{i+1} = [ML]_{eq}^{i} + [H{-}ML]_{eq}^{i} \quad (5)$$

i is the aliquot number. From a first guess for [L], the values of [HL] and $[H_2L]$ were calculated using K_1 and K_2. Combination of eq 4 and K_{M-HL} gave [M] and [M−HL]. Equation 3 then gave [H−ML], while [ML] was obtained from eq 5. A comparison between experimental and calculated (eq 2) values of $[L]_{tot.}$ allowed optimization of [L], as described above for $[H]_{tot.}$. Hereafter, K_{H-ML} was calculated for every curve in Figure 1 and the average log K_{H-ML} value for all curves was used to calculate K_{M-HL}, since these constants are related *via* eq 6.

$$\beta_{MHL} = [MHL]/[M][H][L] = ([M{-}HL] + [H{-}ML])/[M][H][L]$$
$$= K_{M-HL}K_{HL} + K_{H-ML}K_{ML} = \beta_{M-HL} + \beta_{H-ML} \quad (6)$$

This new estimate for K_{M-HL} was used to recalculate the speciation in exactly the same manner until its value no longer changed. The resulting K_{H-ML} values for all curves were in a close range (log K_{H-ML} = 5.2 ± 0.2).

The pH_0 values for the potentiometric formation experiments shown in Figure 4 were obtained as follows. Starting with first guesses for

(11) Huskens, J.; Van Bekkum, H.; Peters, J. A. *Comput. Chem.* **1995**, *19*, 409−416.
(12) Van Westrenen, J.; Khizhnyak, P. L.; Choppin, G. R. *Comput. Chem.* **1991**, *15*, 121−129.

Table 1. Initial Conditions ($t = 0$) for the Potentiometric Titration of 2.7 mM NOTMP + 3.0 mM Mg^{II} with 0.1 M HCl ($I = 0.1$ M KCl, 298 K) for the Kinetic Model Shown in Scheme 1

$[H_{tot.}]/[L_{tot.}]$	pH_0	$[ML]_0$, mM	$[M]_0$, mM	$[L]_{f,0}$, mM	$[H-ML]_0$, mM	$[M-HL]_0$, mM	$(d(pH)/dt)_0$, 10^{-2} units s^{-1}	$r_{d,0}$, 10^{-6} M s^{-1}	$k_{f,M-HL}[M-HL]_0$, 10^{-6} M s^{-1}
0.19	6.63	2.13	0.48	0.21	0.29	0.01	1.58	3.3	0.02
0.30	6.31	1.84	0.75	0.48	0.29	0.02	1.17	4.4	0.04
0.41	6.16	1.55	1.00	0.73	0.29	0.05	0.88	4.0	0.10
0.52	5.97	1.27	1.26	0.98	0.28	0.08	0.77	4.4	0.16
0.63	5.70	1.00	1.50	1.22	0.27	0.11	0.73	5.8	0.22
0.74	5.39	0.75	1.74	1.46	0.25	0.15	0.71	6.3	0.30
0.85	5.12	0.47	1.97	1.68	0.24	0.19	0.52	6.2	0.38

Table 2. Equilibrium Conditions for the Potentiometric Titration of 2.7 mM NOTMP + 3.0 mM Mg^{II} with 0.1 M HCl ($I = 0.1$ M KCl, 298 K) for the Kinetic Model Shown in Scheme 1

$[H_{tot.}]/[L_{tot.}]$	pH	[ML], mM	[M], mM	$[L]_f$, mM	[H−ML], mM	[M−HL], mM	$k_{d,H-ML}[H-ML]$, 10^{-6} M s^{-1}
0.19	7.94	2.13	0.74	0.48	0.003	0.02	0.04
0.30	7.65	1.84	1.00	0.73	0.006	0.05	0.08
0.41	7.39	1.55	1.25	0.98	0.010	0.08	0.14
0.52	7.16	1.26	1.49	1.22	0.014	0.11	0.20
0.63	6.95	0.97	1.72	1.46	0.019	0.15	0.27
0.74	6.73	0.68	1.95	1.68	0.025	0.20	0.35
0.85	6.48	0.40	2.16	1.89	0.032	0.25	0.45

[L] and [H], the values of [HL] and $[H_2L]$ were calculated using K_1 and K_2. Subtraction of eq 2 from eq 1 gave [M], and combination with K_{M-HL} provided [M−HL]. Combination of eq 5 with K_{H-ML} gave [ML] and [H−ML]. Comparison between experimental and calculated values of $[L]_{tot.}$ and $[H]_{tot.}$ allowed simultaneous optimization of [L] and [H], as described above. The resulting [H] values were translated into pH_0.

The kinetic simulations of Figures 1 and 4, as well as the free ligand fractions obtained from the NMR experiments, were performed as follows. Conditions for the $(i+1)$st aliquot of titrant at $t = 0$ are given by eqs 7−9 (dilution effects are omitted for clarity), where H_{add} is the

$$[M_{tot.}]^{i+1} = [M_{tot.}]^{i} \quad (7)$$

$$[L_{tot.}]^{i+1} = [L_{tot.}]^{i} \quad (8)$$

$$[H_{tot.}]^{i+1} = [H_{tot.}]^{i} + [H]_{add} \quad (9)$$

increase or decrease of the proton balance due to the addition of HCl or KOH, respectively. Making the assumption that no reaction had started at $t = 0$ leads to eqs 4 and 5. All species concentrations at $t = 0$ were obtained as described above. The change of the speciation with time was evaluated by starting from first guesses for [ML], [L], and [H]. The protonation constants were used to calculate [HL] and $[H_2L]$, while [H−ML] was derived from K_{H-ML}. For simulation of the curves of Figure 1, the K_{H-ML} value obtained separately for each curve was used, since it influenced the calculated value of pH_0 (but not the initial slopes). For the upper two curves in Figure 1, it was required to increase pH_0 slightly above the values estimated by extrapolation to obtain a better fit between experimental and calculated curves. For all other simulations, the average log K_{H-ML} value was used. The change in sum of [M] and [M−HL] (which species are in rapid equilibrium) with time is given by eq 10 (for description and

$$[M]_{t+\Delta t} + [M-HL]_{t+\Delta t} = [M]_t + [M-HL]_t + (k_{d,ML}[ML]_{av} + k_{d,H-ML}[H-ML]_{av} - k_{obs,i}[M]_{av}[L]_{av} - k_{f,M-HL}[M-HL]_{av})\Delta t \quad (10)$$

determination of the kinetic constants: see text). Here, the subscript "av" indicates average concentrations between t and $t + \Delta t$, using a linear estimate of concentrations ($[S]_{av} = ([S]_t + [S]_{t+\Delta t})/2$).[11] Combination with K_{M-HL} gave [M] and [M−HL], after which comparison between the calculated and experimental values of the mass balances given in eqs 1−3 provided better estimates for [ML], [L], and [H], respectively. Thus, the speciation and the kinetics were optimized simultaneously, as discussed before.[11] The simulation of Figure 4 was used to optimize $k_{obs,i}$ for every curve separately.

Results

Dissociation Kinetics of Mg(NOTMP). The dissociation kinetics of Mg(NOTMP) was studied by nonequilibrium potentiometry by consecutively adding equal aliquots of 0.1 M HCl to a solution of 2.7 mM NOTMP also containing a small excess of KOH and $MgCl_2$. The pH was monitored as a function of time until the change in pH was less than 0.02 units/min. Figure 1 shows the pH curves, obtained from top to bottom, as a function of the $[H]_{tot.}/[L]_{tot.}$ ratio ($[H]_{tot.}$, $[L]_{tot.}$: total proton and ligand concentration, respectively; L = NOTMP). Upon the addition of each aliquot of HCl the pH dropped more than one unit, after which the pH increased until a new equilibrium value was reached. Preliminary titrations of KOH with HCl showed that mixing of the cup solution and equilibration of the electrode took about 10 s. Therefore, pH readings were recorded 15 s after mixing and continuously until equilibrium was reached.

Figure 1 shows some interesting features. Equilibration was slower at lower pH values, as expected, and the pH difference between the first and last reading was invariantly about 1 pH unit. Furthermore, the initial slopes of the curves during the first 1−2 min were similar, especially those curves that began with an initial pH > 5.5.

These dissociation data were used to establish a kinetic model. In all evaluations discussed below, it was assumed that mixing was rapid and ideal, *i.e.* that it did not influence the reaction kinetics. Since the highest protonation constant of L (10.92) is much higher than the pH range shown in Figure 1, while the second (3.97) and third (2.05) constants are much lower, the free ligand was present predominantly as HL. If the formation of protonated complexes is excluded, the rate determining step can be assumed to be the dissociation of ML. According to this model, addition of HCl (increase of $[H]_{tot.}$) can only lead to protonation of HL or an increase in [H] (*i.e.* decrease of pH). For the first few curves at low $[H]_{tot.}/[L]_{tot.}$, [HL] is small because ML is formed to a large extent, so the initial pH drop should have been largest (about 4 pH units) after the first addition of acid and smaller for each subsequent addition (to about 1.6 pH units for the last aliquot of acid). Clearly, this was not supported by the data. Furthermore, it was evident that the initial pH drop after the first addition of acid was smaller than predicted by this model (only about 1.3 pH units), indicating that H^+ is taken up by a species other than HL under these conditions. The complex was the only remaining species present that could be protonated.

The fit of the pH titration curves for Mg(NOTMP) indicated[6] that a minor monoprotonated species, MHL, was present at equilibrium below pH 8 with an overall stability constant β_{MHL} ($\log \beta_{MHL} = 12.76 \pm 0.15$). This could have been a species H−ML, which we suggest to be the reactive species in this dissociation, a species M−HL, or a mixture of both. The former complex is formed by protonation of the complex ML, while the latter is an adduct of M and HL in which M is only partially coordinated to the ligand and the proton is bound to a ring N-atom. As will be shown below, the latter species is involved in the formation pathway. A thermodynamic study[13] of Mg-

(13) Bevilacqua, A.; Gelb, R. I.; Hebard, W. B.; Zompa, L. J. *Inorg. Chem.* **1987**, *26*, 2699−2706.

Scheme 1

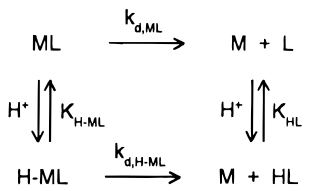

(NOTA) and MgH(NOTA) (NOTA = 1,4,7-triazacyclononane-1,4,7-triacetate) showed that the proton in the latter complex was bound to a N-atom of the ring and that the metal ion was bound to the acetate groups. Thus, in the case of MgH(NOTA), the species M−HL is the only or major form with overall stoichiometry MHL present under equilibrium conditions.

Inclusion of both M−HL and H−ML as possible (kinetic) species leads to a model, in which the species H−ML is formed rapidly by protonation of ML, and rearranges and dissociates slowly to HL and M, while M−HL is formed rapidly by complexation of M and HL. Scheme 1 summarizes the model which incorporates dissociation of ML and of H−ML. The mass balances for this model are given in eqs 1−3. The reaction rate (eq 11) can be described by the kinetic parameters, $k_{d,ML}$

$$r_d = -d([H-ML] + [ML])/dt \quad (11)$$

$$r_d = k_{d,ML}[ML] + k_{d,H-ML}[H-ML] = [ML](k_{d,ML} + k_{d,H-ML}K_{H-ML}[H]) = k_{d,obs}[ML] \quad (12)$$

and $k_{d,H-ML}$, for the dissociation of ML and H−ML, respectively, and the equilibrium constant, $K_{H-ML} = [H-ML]/[H][ML]$, according to eq 12. To obtain K_{H-ML}, all species concentrations at $t = 0$ (left portion of Table 1) and at equilibrium (left portion of Table 2) after each addition of titrant were evaluated from the mass balances (eqs 1−3) by an iterative procedure outlined above and discussed previously,[11] using the extrapolated pH_0 values and the protonation constants of L and HL ($\log K_1 = 10.92$, $\log K_2 = 3.97$).[6] The iterative procedure allowed optimization of both K_{M-HL} and K_{H-ML} for each curve of Figure 1. The values of $\log K_{H-ML}$ and $\log K_{M-HL}$ were in a close range (5.2 ± 0.2 and 1.79 ± 0.10, respectively), which strongly supports the validity of this model. Given that $\log K_{ML} = 6.66$,[6] $\log \beta_{M-HL} = 12.71$ and $\log \beta_{H-ML} = 11.8$ can be estimated from eq 6. Thus, under equilibrium conditions, M−HL is about 8 times more abundant than H−ML (see also Table 2), which is in agreement with the observations reported previously for MgH(NOTA).[13] Under the initial conditions of the dissociation experiment described here, however, H−ML is more abundant than M−HL (see Table 1). Two points remained to be elucidated: (i) Does the initial pH change rate, $(d(pH)/dt)_0$, correspond to the rate law given by this model, and (ii) can the model explain the constant pH change rate observed during the first few minutes?

To evaluate the kinetic parameters, $k_{d,ML}$ and $k_{d,H-ML}$, a relationship between the initial pH change rate, $(d(pH)/dt)_0$, and the initial dissociation rate, $r_{d,0}$, had to be established. A general formula for the initial dissociation rate is given by eq 13 (see

$$r_{d,0}(ab - 1) = \ln(10) \times ([ML]_0 + b[H]_0 + b(2 - a - K_{M-HL}(a - 1))[H_2L]_0)(d(pH)/dt)_0 \quad (13)$$

Supporting Information). Here, the subscript 0 refers to $t = 0$, $(d(pH)/dt)_0$ is the initial pH change rate, $a = (1 + 2K_2[H]_0 + K_{M-HL}([M]_0 + (1 + K_2[H]_0)[HL]_0))/(1 + K_2[H]_0 + K_{M-HL}([M]_0 + (1 + K_2[H]_0)[HL]_0))$, and $b = 1 + 1/(K_{H-ML}[H]_0)$. The initial rates obtained by this equation are listed in Table 1 (right portion). Plotting $k_{d,obs}$ (see eq 12) *vs* $[H]_0$ (Figure 2) gave a straight line with $k_{d,H-ML}K_{H-ML}$ as the slope (2040 ± 93 M^{-1} s^{-1}) and $k_{d,ML}$ as the intercept ($(6 \pm 4) \times 10^{-4}$ s^{-1}). From the slope, $k_{d,H-ML} = (1.4 \pm 0.1) \times 10^{-2}$ s^{-1} was derived. Since the intercept was small, it was concluded that spontaneous dissociation of ML did not contribute significantly to the initial dissociation rates.

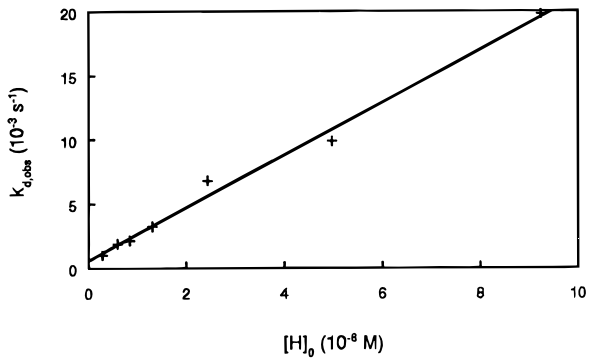

Figure 2. Values of $r_{d,0}[H]_0/[H-ML]_0$ *vs* $[H]_0$ for the potentiometric dissociation experiment.

Between pH 6 and 8, a relation between the rate of pH change and the rate constant $k_{d,H-ML}$ can be easily derived (see Supporting Information), as shown in eq 14. This equation

$$d(pH)/dt = k_{d,H-ML}/\ln(10) \quad (14)$$

clearly shows not only that the rate of pH change is constant in time (in this pH range, and as long as the formation rate is negligible), but also that this rate should be about the same for all curves shown in Figure 1. The lower pH rates for the lowest curves (with $pH_0 < 6$) can be attributed to significant contributions of $[H_2L]$ and [H], so that the simplifications used for eq 14 are not valid under these conditions.

Under equilibrium conditions, proton assisted dissociation ($r_{d,H-ML} = k_{d,H-ML}[H-ML]$; see right portion of Table 2) was considerably slower than the initial rates in the dissociation experiments, due to decrease of [H−ML]. It is, therefore, unclear if spontaneous dissociation of ML contributes significantly at equilibrium or not. The evaluation given above for the dissociation experiments (intercept of Figure 2) indicates that $k_{d,ML}$ has an upper limit of about 1×10^{-3} s^{-1}.

An NMR titration experiment was also performed to observe dissociation of the complex. In this case, larger aliquots of acid were used, providing three data sets of species concentrations as a function of time. As described before,[6] NOTMP and Mg(NOTMP) are in slow exchange on the NMR time scale, thus producing two separate resonances in the ^{31}P NMR spectrum at 37.0 and 42.5 ppm, respectively. The peak areas provide their relative concentrations. The spectra for the first data set ($[H]_{tot.}/[L]_{tot.} = 0.43$) are shown in Figure 3. Every spectrum consist of eight scans collected over a period of 10 s. It was assumed that this period was short enough to provide an accurate estimate of [NOTMP] and [Mg(NOTMP)].

Figure 3 shows that the chemical shift and the line widths of both the free ligand and the complex resonance do not change substantially with time. Only for the third data set ($[H]_{tot.}/[L]_{tot.} = 0.92$) was the chemical shift of the free ligand about 0.1 ppm higher in the beginning, indicating partial protonation of HL to H_2L.[6] The data in Table 1 show that the ratio $[H-ML]_0/[ML]_0$ ranged from 0.14 to about 0.51. This indicates that the protonation of ML to H−ML does not alter the ^{31}P chemical shift of the Mg(NOTMP) resonance. The free ligand fractions, as obtained from measuring the relative peak areas, agreed with the potentiometric data discussed above (see Supporting Information).

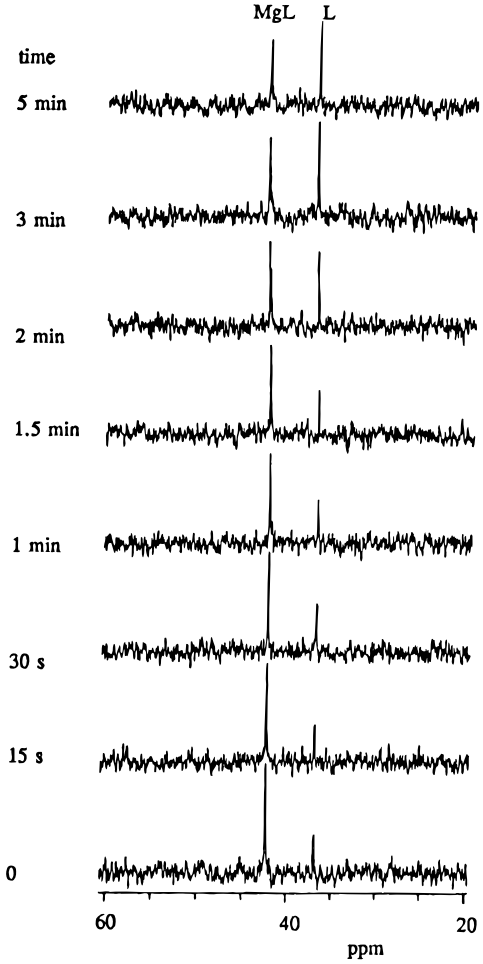

Figure 3. ^{31}P NMR spectra (202 MHz, 298 K) for the titration of 2.7 mM NOTMP + 3.0 mM Mg^{II} with 0.1 M HCl at $[H]_{tot.}/[L]_{tot.} = 0.43$ as a function of time.

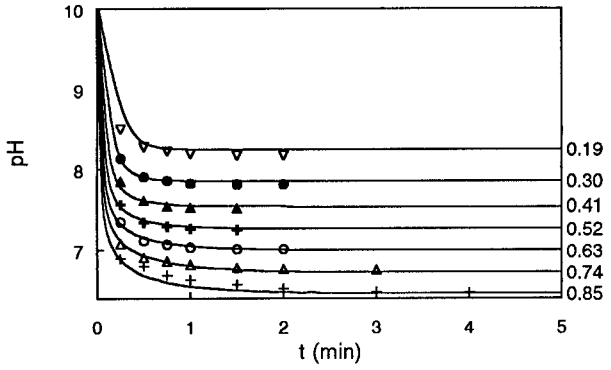

Figure 4. pH *vs* time as a function of $[H]_{tot.}/[L]_{tot.}$ (values shown next to corresponding curves) for the potentiometric titration of 2.7 mM NOTMP + 3.0 mM Mg^{II} with 0.1 M KOH (I = 0.1 M KCl, 298 K). The solid lines were obtained by simulation of the kinetic model shown in Scheme 3.

Formation Kinetics of Mg(NOTMP). Analogous to the dissociation experiment, a NOTMP solution containing excess HCl and $MgCl_2$ was titrated with KOH to study the formation kinetics. The resulting pH curves (Figure 4) show that equilibrium was reached significantly faster (2−3 min) than for the dissociation experiments (Figure 1; 3−10 min), while the equilibration for the former appeared to be less pH sensitive than for the latter. Since no pH data could be collected for the first 15 s, extrapolation to $t = 0$ was not attempted. However, the initial pH values (pH_0) can be estimated using the same technique as discribed above for the dissociation experiment, assuming that no complex formation has taken place and that

Scheme 2

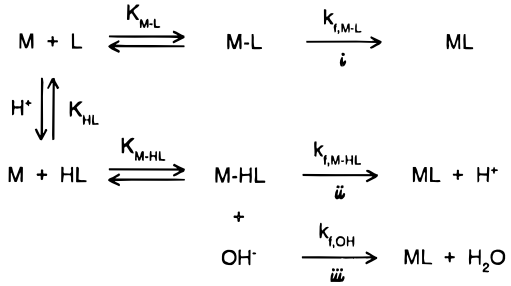

no hydroxy species are formed. The last assumption is justified, since the log K value[14] for Mg(OH) is only about 2.5. This indicates that formation of Mg^{II} hydroxide species only takes place appreciably above pH 11. The pH_0 values obtained by this procedure ranged from 9 to 10, indicating that the initial pH changes were quite rapid.

For the formation kinetics we propose three possible pathways: (i) rapid formation of an intermediate M−L (in which M is only partially coordinated by L) that slowly rearranges to the final complex ML, (ii) rapid formation of an intermediate M−HL that slowly rearranges (with consecutive deprotonation) to ML in a spontaneous manner, or (iii) rapid formation of M−HL that slowly rearranges to ML *via* a hydroxide-assisted pathway (see Scheme 2).

The stability of the intermediate M−HL was determined as described above (log $K_{M-HL} = 1.79$). Since its concentration is maximally about 10% of the ligand mass balance under equilibrium conditions, it is easily seen that its contribution to the mass balances of eqs 1−3 will be negligible at all times during the formation experiments since the pH is continuously higher than the equilibrium value, leading to smaller concentrations of HL. Since [L] will be small at pH < 10, the concentration of the intermediate M−L can also be ignored. Thus, the rate equations for pathways i−iii in Scheme 2 can be written as eqs 15−17. Pathway ii is complimentary to the

$$r_{f,i} = k_{f,M-L}[M-L] = k_{f,M-L}K_{M-L}[M][L] = k_{obs,i}[M][L] \quad (15)$$

$$r_{f,ii} = k_{f,M-HL}[M-HL] = k_{f,M-HL}K_{M-HL}[M][HL] = k_{obs,ii}[M][HL] \quad (16)$$

$$r_{f,iii} = k_{f,OH}[M-HL][OH] = k_{f,OH}K_{M-HL}K_wK_1[M][L] = k_{obs,iii}[M][L] \quad (17)$$

proton assisted dissociation pathway given above. Therefore, $k_{obs,ii}$ (0.12 M^{-1} s^{-1}) can be calculated from equilibrium conditions using eq 18, which leads to $k_{f,M-HL} = 2.0 \times 10^{-3}$

$$k_{obs,ii} = k_{d,H-ML}K_{H-ML}K_{ML}/K_1 \quad (18)$$

s^{-1}. This rate constant is too low, however, to explain the pH curves shown in Figure 4. So, either pathway i or iii must also contribute. Equations 15 and 17 show that discrimination between these pathways cannot be accomplished from the pH curves of Figure 4 alone, since their overall rate laws are equal. The most elegant solution to this problem is to perform a second titration using D_2O as solvent.[15] If pathway i is involved, the observed rate constant ($k_{obs,i}$) should not change, while in

(14) Martell, A. E.; Smith, R. M.; Motekaitis, R. J. *NIST Critical Stability Constants of Metal Complexes Database, NIST Standard Reference Database 46*; NIST: Gaithersburg, MD, 1993.
(15) Wu, S. L.; Horrocks, W. DeW., Jr. *Inorg. Chem.* **1995**, *34*, 3724−3732.

Scheme 3

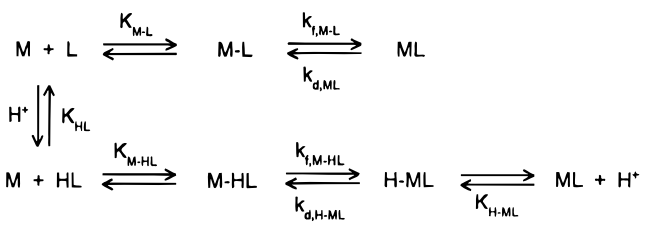

pathway iii $k_{obs,iii}$ is dependent on K_w which is about 18 times smaller in D_2O than in H_2O. A titration in D_2O, performed identically to the one in H_2O described above, provided pH curves similar to those in Figure 4 (see Supporting Information).

The spreadsheet approach discussed earlier[11] was used to calculate pH curves as a function of $k_{obs,i}$. A least-squares approach was used to obtain a $k_{obs,i}$ value for every pH curve of Figure 4. Averaging led to a value for $k_{obs,i}$ (or $k_{obs,iii}$) of $(1.0 \pm 0.1) \times 10^3$ M^{-1} s^{-1} in H_2O and of $(0.8 \pm 0.2) \times 10^3$ M^{-1} s^{-1} in D_2O. This shows that the observed rate constants are not significantly different in H_2O and D_2O. Therefore, we conclude that pathway i, and not iii, is the one observed in our case. A similar reasoning as given above for the proton-assisted pathway under equilibrium conditions can be made for the spontaneous formation/dissociation pathway, leading to a value for $k_{d,ML}$ of 2×10^{-4} s^{-1}, using eq 19. This value certainly

$$k_{d,ML} = k_{obs,i}/K_{ML} \tag{19}$$

meets the requirement set by the upper limit (1×10^{-3} s^{-1}) as discussed earlier.

NMR titrations in both H_2O and D_2O were performed to study the formation kinetics, similar to that shown above for the dissociation reaction. In contrast to Figure 3, an abrupt change in the ratio of the two peaks was observed from the first ($t = 0$) to the second ($t = 0.25$ min) spectrum, after which the ratio no longer changed. No chemical shift changes were observed. This agrees well with a simulation (see Supporting Information) using the formation pathways i and ii presented above, which shows that the formation of ML is more than 95% complete within that time period.

Complete Kinetic Model. All curves drawn through the data points in Figures 1 and 4, as well as the free ligand fractions obtained from the NMR experiments (see Supporting Information), were simulated with a spreadsheet program outlined above and described previously[11] using the stability constants determined before[6] and the rate constants given above. The overall kinetic scheme is shown in Scheme 3. In the proton-assisted pathway, the interconversion between H−ML and M−HL is shown as a single rate-determining step. It can not be excluded, however, that there are two parallel pathways, one between M−HL and ML, and the other between HL and H−ML.

The model is capable of predicting all curves of Figures 1 and 4 reasonably well. The linear parts for the pH curves in Figure 1 are correctly predicted, while the lower rate for the lowest curve is attributed to the presence of $[H_2L]$ (see above). Only the initial slopes for the upper two curves were not well predicted; the experimental slopes were higher than the calculated values. The data in Figure 4 were also well described by the model, while the data obtained in D_2O did not fit as well (see Supporting Information), probably because all of the stability constants are somewhat different in D_2O. This was already expressed in the higher standard deviation of $k_{obs,i}$ in D_2O compared to H_2O. Although the scatter of the NMR data is quite large due to the short accumulation times of the spectra, the fit of these data to the model also appeared to be reasonably good.

With the value for $k_{f,M-HL}$, it can easily be shown that the proton-assisted formation contributes only up to 6% of the observed pH change rate during the initial conditions of the dissociation experiments, as shown by a comparison of $k_{f,M-HL}[M-HL]_0$ with $r_{d,0}$ (Table 1). This means that the value for $k_{d,H-ML}$ is correctly obtained from the procedure outlined above, and that the aliquots of acid titrant were large enough to suppress the formation sufficiently under these conditions.

As suggested by the results outlined above, the reaction rate for the dissociation experiments was dominated by a proton-assisted pathway, while in the formation experiments the pathway *via* M−L prevailed. This is a pH-dependent phenomenon. A plot of the fraction of the dissociation rate that is determined by the spontaneous dissociation of ML ($= r_{d,ML}/r_d = k_{d,ML}/(k_{d,ML} + k_{d,H-ML}K_{H-ML}[H])$ *vs* pH shows a sigmoidal behavior, in which the fraction is low at low pH, rises to 0.5 at pH 7.0, and approaches unity at high pH (see Supporting Information). At equilibrium, this pH dependence is obviously the same as for the formation reaction. Thus, we conclude that the proton-assisted pathway predominates at pH values below 7.0, while spontaneous dissociation of ML and the formation of ML from M−L prevail above pH 7.0.

Discussion

Structure and Stability of the Intermediate Complexes. The potentiometric titrations provide no direct information about the structure of the intermediates H−ML, M−L, and M−HL. However, the reaction pathways which lead to formation of these species provide some hints. In the proton assisted dissociation pathway, the intermediate H−ML is formed by protonation of the complex, ML. Since the three nitrogen atoms of NOTMP are all coordinated to the Mg^{II} ion in the species ML *via* long-lived bonds and the overall negative charge (1−) of the complex is localized mainly on the phosphinate groups, it is plausible that the initial protonation takes place at one of the phosphinate oxygens or forms a hydrogen bridge between two of them. The magnitude of the protonation constant ($\log K_{H-ML} = 5.2$) suggests hydrogen bridging because it seems too large to involve protonation of a single phosphinate oxygen ($\log K < 3$).[16] Unexpectedly, the ^{31}P chemical shift of the Mg(NOTMP) resonance did not change upon protonation. However, the NMR experiment clearly shows that the intermediate is in fast exchange with the complex and not with the free ligand, which must mean that the (long-lived) Mg^{II}−N bonds are still intact. In the formation experiment, the intermediates M−L and M−HL are formed by binding of the Mg^{II} ion with the fully deprotonated (L) or monoprotonated ligand (HL). Since the proton in HL is at a ring nitrogen and the overall 2− negative charge is localized at the phosphinate groups, it is plausible that the metal ion binds initially to the phosphinate groups only to give M−HL. It is likely that a similar reasoning holds for the intermediate M−L. Then, in a slow step, these intermediates rearrange to point the N lone pairs toward the metal ion, for M−HL probably simultaneous with deprotonation. Since the complex formation went too fast to be followed by NMR and the amounts of M−L and M−HL were too low to have a significant contribution to the mass balances, the spectra for these experiments did not give more information about the structure of these intermediates.

Protonated complexes of overall composition MHL have often been observed, also under equilibrium conditions. The assignment of this complex as M−HL or H−ML is then not

(16) pK_as of phosphinate groups in macrocyclic compounds were observed to be about 2 (see ref 6 and Van Haveren, J.; DeLeon, L.; Ramasamy, R.; Van Westrenen, J.; Sherry, A. D. *NMR Biomed.* **1995**, *8*, 197−205); the pK_a of other similar compounds are for example: 1.1 for $H_2P(O)OH$ and 1.0 for $(BuO)_2P(O)OH$ (see ref 14).

straightforward, but has sometimes been deduced from thermodynamic data. For example, the Mg^{II} ion in $Mg(NOTA)^-$ seems to be coordinated by only five ligand sites, while the proton in the protonated form MHL appeared to be on a N-atom.[13] It was, therefore, concluded that the Mg^{II} ion in this complex is only coordinated by the acetate groups. This is a clear case where the complex of overall stoichiometry MHL (observed under equilibrium conditions) was in fact a species M−HL, which must mean that here this complex is more stable than H−ML. From their results, a log K_{M-HL} value of 2.6 can be calculated. This shows that NOTA (log K_{ML} = 9.7) and HNOTA (2.6) bind Mg^{II} stronger than NOTMP (6.66) and HNOTMP (1.79), consistent with stronger binding of the acetate *vs* the methylphosphinate groups. In our case, the overall stability constants β_{H-ML} (log β_{H-ML} = 11.8) for H−ML and β_{M-HL} (log β_{M-HL} = 12.71) for M−HL are remarkably close to each other ($\Delta\Delta G$ = 5.2 kJ/mol), while their structures are very different. In agreement with the study on MgH(NOTA),[13] M−HL is the predominant species under equilibrium conditions compared to H−ML. Since the *K* value of Mg(IDA) (IDA = iminodiacetate) is much higher (log *K* = 3)[14] than the stability of M−HL, we conclude that Mg^{II} is bound only to the phosphinate groups in the M−HL species.

The formation constant of an outer sphere complex between a divalent cation (Mg^{2+}) and a divalent anion (HL^{2-}) can be estimated to be 3.3 M^{-1}.[17,18] The actual K_{M-HL} value found here is 62 M^{-1}, which is a factor 19 higher than the outer sphere estimate. Similarly, if we assume that K_{M-L} is also 19 times higher than the outer sphere value for M^{2+} and L^{3-} (13 M^{-1}), values of log K_{M-L} = 2.39 and $k_{f,M-L}$ ($=k_{obs,i}/K_{M-L}$) = 4.1 s^{-1} can then be estimated. Overall, we conclude that protonation of ML accelerates dissociation by a factor 70 ($k_{d,H-ML}/k_{d,ML}$), while monoprotonation of the free ligand at one of the ring nitrogens makes accommodation of Mg^{II} about 2000 ($k_{f,M-L}/k_{f,M-HL}$) times more difficult.

Comparison with Other Kinetic Schemes. Proton-assisted dissociation pathways have been observed for a variety of metal macrocyclic ligand complexes, such as $Ln(NOTA)^0$ (NOTA = 1,4,7-triazacyclononane-1,4,7-triacetate),[19] $Gd(DETA)^0$ (DETA = 1,4,7-triazacyclodecane-1,4,7-triacetate) and analogues,[20] $Cu(DO3A)^-$ and $Ln(DO3A)^0$ (DO3A = 1,4,7,10-tetraazacyclododecane-1,4,7-triacetate),[21,22] and $Gd(DOTA)^-$ (DOTA = 1,4,7,10-tetraazacyclododecane-1,4,7,10-tetraacetate).[23] These studies were performed at low pH (<2) to attain acceptable dissociation rates. Protonated intermediate complexes H_n−ML have often been deduced from the pH behavior of $k_{d,obs}$. The protonation constant (log K_{H-ML}) of ML may depend on the charge of the complex, the nature of the group that is protonated, and the radius of the metal ion. For example, the value for $Gd(DOTA)^-$ is 2.8, while the protonation of the neutral analogs Gd(DO3A) and Gd(HP-DO3A) (HP-DO3A = 1-(2-hydroxypropyl)-1,4,7,10-tetraazacyclododecane-4,7,10-triacetate) is more difficult (2.1 and 2.4, respectively).[22] The dependence of log K_{H-ML} on the radius and charge density of the metal ion for a given ligand may not be as obvious. For example, the log K_{H-ML} value for $Pb(DOTA)^{2-}$ is only 0.6.[24] This indicates that the larger ionic size of Pb^{II} has a greater influence on protonation of the complex than the (larger) overall charge. Perhaps the ability to form hydrogen bridges between more than one protonation site is important here. In our case, H−ML is a species that occurs in measurable concentrations between pH 5 and 7 under nonequilibrium conditions, and a derived pK_a of 5.2 also seems to suggest hydrogen bridging. The formation rate of DOTA with several divalent metal ion complexes was found to correlate with the concentration of HL, even though H_2L was the major ligand species under their conditions.[25] This is analogous to the pathway *via* M−L in this study. For $Eu(DOTA)^-$, however, a hydroxide assisted mechanism *via* M-H_2L has been proven convincingly.[15] In that example, the intermediate could be studied extensively due to the very slow rearrangement to the final complex. The stability of this intermediate was determined, and a large effect on the reaction rate was observed by changing the solvent to D_2O, confirming the involvement of hydroxide in the reaction mechanism. The reaction of the intermediate complex of the metal ion with the major ligand species has been observed,[19−21] but often as a minor component. Stability constants of intermediates M−H_nL were determined in some cases,[15,19,23,26] and were generally 10−100 times larger than the outer sphere estimates. In our case, K_{M-HL} is about 19 times higher than the outer sphere estimate, which agrees quite well with this range.

Conclusions

Nonequilibrium potentiometry is a powerful tool for the investigation of complexation kinetics, which requires no additional indicator or buffering base. Although it provides no direct information about the structure of the reactive intermediates, initial pH data can provide information about the reaction pathway. Furthermore, rates of change of pH may be observed even when changes in concentrations of metal ions and complexes are very small. The system Mg^{II}−NOTMP is an example of a case in which both proton-assisted and spontaneous formation/dissociation take place. It shows that pathways depend on pH: while the formation rate of ML from M−H_nL decreases rapidly with increasing *n*, it depends on the relative concentrations of the several protonated ligand forms H_nL, and thus on the pH, as to which reaction pathway prevails.

Acknowledgment. This research was supported in part by grants from the Robert A. Welch Foundation (AT-584) and the NIH Biotechnology Research Program (P41-RR02584).

Supporting Information Available: Text giving the mathematical derivation of eqs 13 and 14, plots of the free ligand fraction *vs* time for the NMR experiments together with simulated curves, a figure showing the plot of pD *vs* time for the formation experiment in D_2O, and a figure showing the simulation of $r_{d,ML}/r_d$ *vs* pH (6 pages). Ordering information is given on any current masthead page.

IC9602299

(17) Nyssen, G. A.; Margerum, D. W. *Inorg. Chem.* **1970**, *9*, 1814−1820.
(18) Margerum, D. W.; Cayley, G. R.; Weatherburn, D. C.; Pagenkopf, G. K. In: *Coordination Chemistry, Vol. 2*; Martell, A. E., Ed.; ACS Monograph 174; American Chemical Society: Washington, DC, 1978; Chapter 1.
(19) Brücher, E.; Sherry, A. D. *Inorg. Chem.* **1990**, *29*, 1555−1559.
(20) Brücher, E.; Cortes, E.; Chavez, F.; Sherry, A. D. *Inorg. Chem.* **1991**, *30*, 2092−2097.
(21) Cai, H.-Z.; Kaden, T. A. *Helv. Chim. Acta* **1994**, *77*, 383−398.
(22) Kumar, K.; Chang, C. A.; Tweedle, M. F. *Inorg. Chem.* **1993**, *32*, 587−593.
(23) Wang, X.; Jin, T.; Comblin, V.; Lopez-Mut, A.; Merciny, E.; Desreux, J. F. *Inorg. Chem.* **1992**, *31*, 1095−1099.
(24) Kumar, K.; Magerstädt, M.; Gansow, O. A. *J. Chem. Soc., Chem. Commun.* **1989**, 145−146.
(25) Kasprzyk, S. P.; Wilkins, R. G. *Inorg. Chem.* **1982**, *21*, 3349−3352.
(26) Kumar, K.; Tweedle, M. F. *Inorg. Chem.* **1993**, *32*, 4193−4199.